Short Chain Branching Effect on the Cloud-Point Pressures of Ethylene Copolymers in Subcritical and Supercritical Propane

S. J. Han,*,† D. J. Lohse,† M. Radosz,‡ and L. H. Sperling§

Exxon Research and Engineering Company, Route 22 East, Annandale, New Jersey 08801, Department of Chemical Engineering and Macromolecular Studies Group, Louisiana State University, Baton Rouge, Louisiana, 70803-7300, and Departments of Chemical Engineering, and of Materials Science and Engineering, Center for Polymer Science and Engineering, Polymer Interfaces Center, and Materials Research Center, Lehigh University, Bethlehem, Pennsylvania 18015-3194

Received October 28, 1997; Revised Manuscript Received February 6, 1998

ABSTRACT: The cloud-point pressures of copolymers of ethylene with propylene, butene, hexene, and octene in propane were measured with a variable-volume optical batch cell to investigate the effects of the number and length of branches on the phase behavior in the temperature range from 25 to 200 °C and at pressures up to 700 bar. As the degree of branching increased in the ethylene−propylene copolymers, ethylene−butene copolymers, and ethylene−hexene copolymers, the cloud-point pressures decreased. At the same degree of branching, the cloud-point pressures decreased slightly upon increasing branch length. The copolymer SAFT (statistical association fluid theory) equation of state was found to correlate the experimental cloud-point data by adjusting the branch segment energy.

Introduction

Since the early development of polyethylene technology, understanding its phase behavior in solution has been crucial to guide the commercial production of polyethylene. For example, phase behavior studies are required for the control of the polymerization reactor, the design of separation operations, and other processing applications. However, the phase behavior of solutions of polyethylene is not well understood because of the complex effects of several molecular variables, including polydispersity, short chain branching, and long chain branching. Spahl and Luft studied the phase behavior of branched low-density polyethylene in ethylene.[1] They found that the cloud-point pressures decreased with increasing branchiness of the polymer. Chen et al. demonstrated the effect of ethyl branches on the cloud-point pressure of hydrogenated polybutadiene in propane.[2] An increase in the number of ethyl branches enhanced miscibility. De Loos et al. reported the influence of branching on high-pressure vapor−liquid equilibria of polyethylene in ethylene.[3] The cloud-point curves of a system with a branchy polyethylene were significantly lower than the cloud-point curves of a system with a linear polyethylene. Charlet and Delmas measured the lower critical solution temperature (LCST) of ethylene−propylene copolymers with varying propylene comonomer content in C5−C9 alkanes.[4] They found that the LCST increased as the ethylene content decreased. Whaley et al. reported cloud-point pressures of branched polyolefins in propane.[5] The cloud-point pressures decreased with increasing octene content for a series of ethylene−octene copolymers.

The development of single-site metallocene catalysts has introduced a new family of polyethylenes, the so-called metallocene linear low-density polyethylene (mLLDPE).[6,7] Metallocene catalysts enable not only improved control of short chain branching but also narrower molecular weight distribution and more uniform composition distribution than those of polyethylene synthesized with Ziegler catalysts or free radical initiators. The physical properties of mLLDPE can be fine-tuned by the control of the incorporation of comonomers (e.g., propylene, 1-butene, 1-hexene, 1-octene) during the polymerization of ethylene, which results in the introduction of short chain branches onto the polyethylene backbone.

The objective of this paper is to understand the effect of such short chain branching on the cloud-point pressures of the metallocene-catalyzed ethylene copolymers, in subcritical and supercritical propane solutions. The approach involves measuring the cloud-point pressures of the copolymers in propane solutions at constant composition in a variable volume optical batch cell and then correlating the experimental cloud-point pressures with an equation of state model.

SAFT Modeling

The experimentally measured cloud points were correlated using the copolymer SAFT equation of state, which extended the original SAFT model by treating heterobonded polymer chains using the thermodynamic perturbation theory of the first order.[8]

The SAFT residual Helmholtz free energy, a^{res}, is given by

$$a^{res} = a^{hs} + a^{chain} + a^{assoc} + a^{disp} \qquad (1)$$

where a^{res} is a sum of the Helmholtz free energy contributions from hard sphere, chain, association, and dispersion. Since the polymers in this study do not exhibit a specific interaction such as hydrogen bonding, the a^{assoc} term is equal to zero. The a^{chain} term is revised in the copolymer SAFT equation of state by Banaszak et al.,[10] and the other terms are given by Huang and Radosz.[11]

* Corresponding author. Tel: (908) 730-3770. Fax: (908) 730-3313. E-mail: sjhan@erenj.com.
† Exxon Research and Engineering Co.
‡ Louisiana State University.
§ Lehigh University.

S0024-9297(97)01579-9 CCC: $15.00
Published on Web 03/26/1998

Table 1. Characteristics of the Ethylene Copolymers

sample code[a]	branch/100 ethylene units in the backbone	M_w	M_w/M_n	T_m, °C	solubility parameter at 166 °C, MPa$^{1/2}$	source
PE1	0	32 100	1.2	134	n/a[b]	NIST1483
PE2	0	119 600	1.2	n/a	n/a	NBS1484[c]
EP9	8.7	71 000	2.2	113	17.84	metallocene
EP10	10.3	72 500	2.1	89	17.71	metallocene
EP28	28.3	62 800	2.3	30	17.49	metallocene
EP100	100	91 000	2.0	161	16.40	metallocene
EB5	5.3	104 900	2.0	112	18.21	metallocene
EB8	7.5	76 700	2.0	108	18.08	metallocene
EB9	8.8	94 900	1.9	98	17.79	metallocene
EB16	15.9	79 000	1.9	77	17.59	metallocene
EB18	18.0	58 100	2.0	62	17.70	metallocene
EB23	23.3	87 200	1.1	46	17.32	HPB[d]
EB60	60	87 800	1.1	amorphous	17.28	HPB
EH3	2.6	93 200	2.2	128	18.17	metallocene
EH5	4.6	100 800	1.9	118	18.02	metallocene
EH13	13.0	72 300	3.0	76	17.69	metallocene
EO8	7.6	93 600	2.3	104	17.52	metallocene

[a] Sample code = number of branches (methyl for EP, ethyl for EB, butyl for EH, hexyl for EO) per 100 ethylene units in the backbone. PE: linear polyethylene homopolymer. [b] n/a: not available. [c] Data from Condo et al.[14] [d] HPB: hydrogenated polybutadiene.

Table 2. Bond Fractions and Segment Fractions for the Ethylene Copolymers

sample code	backbone−backbone bond fraction	backbone−branch bond fraction	branch−branch bond fraction	backbone segment fraction	branch segment fraction
PE1	1	0	0	1	0
PE2	1	0	0	1	0
EP9	0.957	0.043	0	0.957	0.043
EP10	0.952	0.048	0	0.952	0.048
EP28	0.877	0.123	0	0.877	0.123
EP100	0.666	0.334	0	0.667	0.333
EB5	0.952	0.024	0.024	0.952	0.048
EB8	0.930	0.035	0.035	0.930	0.070
EB9	0.918	0.041	0.041	0.919	0.081
EB16	0.862	0.069	0.069	0.862	0.138
EB18	0.846	0.077	0.077	0.848	0.152
EB23	0.812	0.094	0.094	0.813	0.187
EB60	0.624	0.188	0.188	0.625	0.375
EH3	0.943	0.014	0.043	0.943	0.057
EH5	0.909	0.023	0.068	0.909	0.091
EH13	0.793	0.052	0.155	0.943	0.057
EO8	0.806	0.032	0.162	0.806	0.194

The versatility of the SAFT model and other lattice-cell based equations of state such as the Flory−Huggins theory, the Flory−Orwoll−Vrij theory, and the Sanchez−Lacombe theory is compared by Condo and Radosz.[9] Also, Chen et al.[12] applied SAFT and lattice equations of state to correlating polymer *PVT* data.

The SAFT parameters required for the ethylene copolymers are the temperature independent segment volume (u^{00}) in milliliters per mole of segment, the segment number (m), the backbone segment energy $(u^0/k)_{BB}$ (where k is Boltzmann's constant), and the branch segment energy $(u^0/k)_{BR}$. Copolymer SAFT also requires specific types of bond fractions to account for the chain heterogeneity, such as backbone-to-backbone, branch-to-branch, and backbone-to-branch fractions. The extent of branching can be reflected by the number fraction of backbone segment and the number fraction of branch segment. These bond fractions and segment fractions were calculated from the mole fraction of branch in the copolymers. The parameters for pure propane were the same as those reported by Huang and Radosz.[11] The value of u^{00} for the polymers was set equal to 12 mL/mol, which is an asymptotic value for long chain hydrocarbons.[11] The values of m and $(u^0/k)_{BB}$ for the polymers were estimated using the empirical formulas for the alkane series:[2,11] Huang et al. found that the segment number m is proportional to molar mass for *n*-alkane and long chain polymers.[11]

$$m = 0.05096M_w \tag{2}$$

where M_w = weight average molecular weight and

$$(u^0/k)_{BB} = 210.0 - 26.886 \exp\{-0.013341m\} \tag{3}$$

All the parameter values used in this work are given in Tables 2 and 3.

The cloud-point pressures were calculated using the macromolecular flash method proposed by Chen et al.[13] They applied a new flash algorithm to solve simultaneously all the equilibrium and material balance equations using a Newton iterative procedure in the framework of block algebra. The residual free energy contributions due to the backbone−segment interactions and due to the branch−segment interactions were estimated as follows. The segment energy for the polymer backbone $(u^0/k)_{BB}$ calculated from eq 2 is rounded off to be constant at 210 K for all polymers, and the segmental volume (u^{00}) was also estimated to be constant at 12.0 mL/mol. On the basis of Banaszak et al.,[10] binary interaction parameter, k_{ij}, for the polymer backbone−solvent and polymer branch−solvent were set equal to 0.022. Then, the branch segment energy was adjusted to fit the experimental cloud-point pressures. These branch segment energies are summarized in Table 3.

Table 3. Copolymer SAFT Parameters for the Ethylene Copolymers and Propane

sample code	m	u^{00}, mL/mol	$(u^0/k)_{BB}$, K	$(u^0/k)_{BR}$, K[a]
PE1	1635.8	12.0	210.0	0
PE2	6094.8	12.0	210.0	0
EP9	3618.2	12.0	210.0	160
EP10	3694.6	12.0	210.0	160
EP28	3200.3	12.0	210.0	160
EP100	4637.4	12.0	210.0	181
EB5	5345.7	12.0	210.0	175
EB8	3908.6	12.0	210.0	175
EB9	4836.1	12.0	210.0	175
EB16	4025.8	12.0	210.0	175
EB18	2960.8	12.0	210.0	175
EB23	4443.7	12.0	210.0	165
EB60	4474.3	12.0	210.0	175
EH3	4749.5	12.0	210.0	180
EH5	5136.8	12.0	210.0	180
EH13	3684.4	12.0	210.0	180
EO8	4769.9	12.0	210.0	185
propane	2.696	13.457	190.03	

[a] Fit to data.

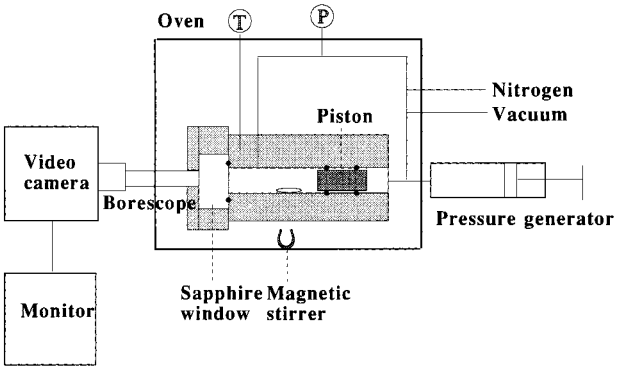

Figure 1. Schematic of the variable volume optical batch cell unit.

Experimental Section

Materials. Most of the polymers used in this work were ethylene copolymers with propylene, butene, hexene, and octene, synthesized with metallocene catalysts. Isotactic polypropylene was also synthesized with metallocene catalyst. The polydispersities of the metallocene polymers were all about 2.0. The linear high-density polyethylenes (PE1, PE2) were purchased from the National Institute of Standards and Technology. Two model EB copolymers (EB23, EB60) with polydispersity of 1.1 were obtained by hydrogenating polybutadiene synthesized with anionic initiator in the presence of polar modifiers to control the vinyl content (1,2 addition of diene).[14] The structure of the polymers was characterized by ^{1}H NMR for the extent of branches, by gel permeation chromatography for the molecular weights of polymers, by differential scanning calorimetry for melting transitions, and by *PVT* measurements for solubility parameter determination.[15] The characteristics of the polymers are summarized in Table 1. The copolymer samples are coded in terms of the number of branches per 100 ethylene repeating units in the polymer backbone, which is equal to the mole percent of comonomer in the ethylene copolymers. Solvent propane (99.9% purity) was obtained from Matheson Gas Co. and used without purification.

Apparatus. The cloud-point pressures of the polymer solutions were determined with a high-pressure variable-volume optical batch cell shown in Figure 1.[16] In brief, a mixture of the polymer and propane of known composition was prepared and then the phase transition of polymer solution was observed visually through a sapphire window in the cell. The polymer solution was pressurized to well above the cloud-point pressure to form a one-phase solution and equilibrated at a constant temperature with stirring. The pressure of the system was then lowered isothermally until the solution became hazy, indicating a liquid−liquid (cloud-point) phase transition. The cloud-point pressure was determined as the pressure at which the solution turned completely cloudy in the cell. For a solid−liquid transition, the homogeneous polymer solution was cooled isobarically until it turned hazy.

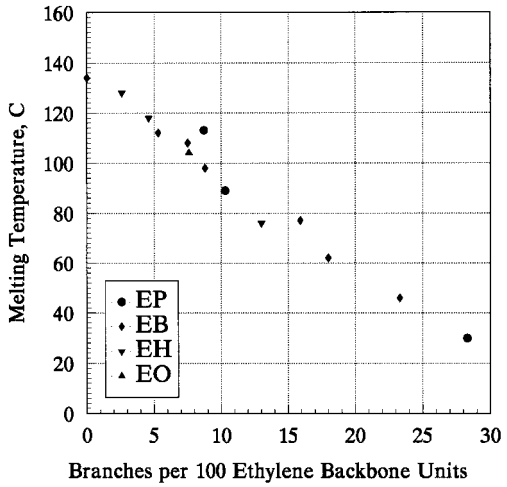

Figure 2. Melting temperatures, T_m, of ethylene copolymers in terms of the number of branches per 100 ethylene backbone units. The scanning rate of the DSC was 10 °C/min.

Results and Discussion

The physical and thermodynamic properties of ethylene copolymers were significantly influenced by the details of the microstructures in the polymer chains. For example, the melting temperatures of ethylene copolymers in terms of number of branches per 100 ethylene backbone units are shown in Figure 2. The melting temperature is taken as the onset temperature at which the last trace of crystallinity disappeared in the DSC thermograms. As the number of branches increased, the melting temperatures decreased monotonically. This is because the short chain branches disrupt the sequence of ethylene unit in the polymer backbone, which limits the crystallizability of polymer chains. As a result, the melting temperatures are reduced as the number of branches increases.

The effect of the branches on the solubility parameter of ethylene copolymer in the melt state is shown in Figure 3. The solubility parameter was calculated from the internal pressure measurement of the polymer, which was determined by the isobaric thermal expansion coefficient and isothermal compressibility.[15] As the number of branches increases, the solubility parameter decreases. This suggests that the effective copolymer interaction energy also decreases as the number of branches increases. Such a decreasing interaction energy is likely to affect the phase behavior of the polymer solutions in small hydrocarbons due to the dissimilar interaction energy between the polymer chains and small molecules.

The cloud-point curves shown in the pressure−temperature phase diagrams from Figure 4 to Figure 11 indicate the minimum pressure required to maintain a homogeneous polymer solution. Therefore, the area above each curve is an one-phase region, and the area below each curve is a two-phase region.

Figure 4 illustrates the pressure−temperature phase diagram for the linear ethylene homopolymers (PE1 and PE2) in propane, which differ in molecular weight. The experimental data for PE2 are taken from Condo.[17] As

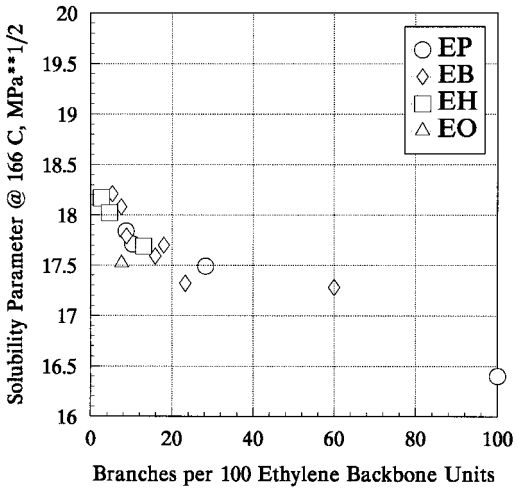

Figure 3. Solubility parameters of ethylene copolymers as determined from internal pressure.

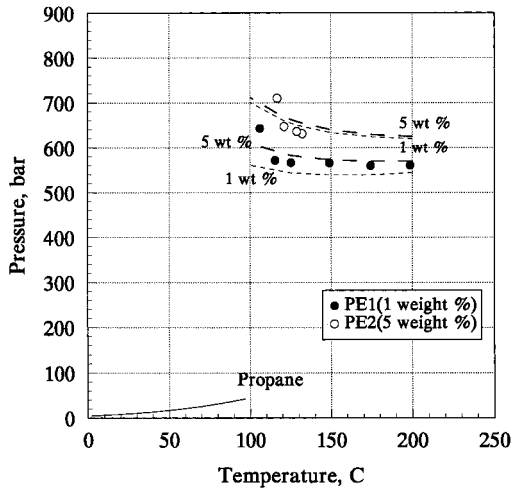

Figure 4. Cloud-point pressures of PE1 and PE2 in propane (1 wt %, 5 wt %). The curves are calculated from the copolymer SAFT equation of state. The solid line is the vapor pressure of propane.

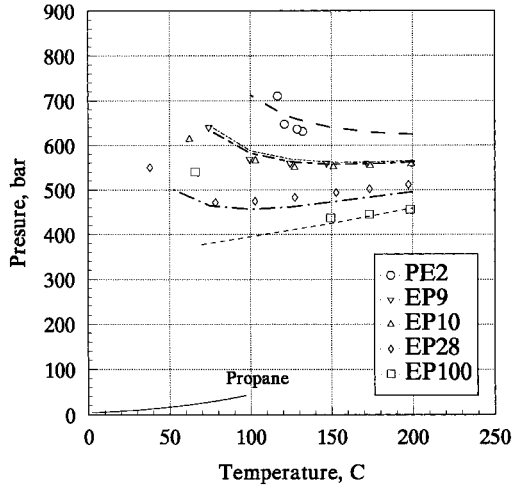

Figure 5. Cloud-point pressures of EP copolymers in propane (5 wt %). The curves are calculated from the copolymer SAFT equation of state. The solid line is the vapor pressure of propane.

the temperature decreases, the cloud-point pressure of those linear polyethylene increases, indicating UCST type phase behavior. The experimental data were

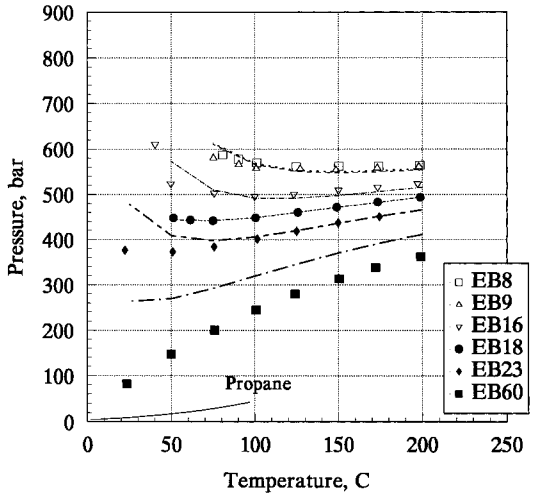

Figure 6. Cloud-point pressure of EB copolymers in propane (1 wt %). The curves are calculated from the copolymer SAFT equation of state. The solid line is the vapor pressure of propane.

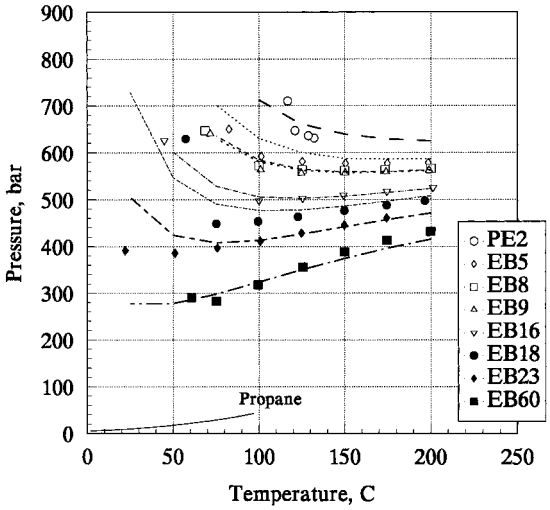

Figure 7. Cloud-point pressure of EB copolymers in propane (5 wt %). The curves are calculated from the copolymer SAFT equation of state. The solid line is the vapor pressure of propane.

correlated with the copolymer SAFT equation of state by setting the solvent−segment binary interaction parameter, k_{ij}, as 0.022 and the branch segment fraction as zero (we assume no branches). As expected, copolymer SAFT predicts the higher cloud-point pressures for the higher molecular weight PE2 in propane and illustrates the polymer concentration effect. For the rest of the polymers, we used the same binary interaction parameter, $k_{ij} = 0.022$, as a universal constant, that is, independent of temperature and polymer molecular weight. Furthermore, we set the branch−solvent parameters to be equal to the backbone−solvent parameter.

The effect of the methyl branches on the cloud-point pressure of the EP copolymers in 5 wt % solutions in propane is shown in Figure 5. As the number of methyl branches increased, the cloud-point pressures decreased. EP100 is an isotactic polypropylene, synthesized with a metallocene catalyst, which shows a solid−liquid transition near 65 °C due to the crystallinity. The solid−liquid transition of the semicrystalline ethylene copolymer solutions is found upon isobaric cooling from a homogeneous solution. Here is the distinction: the

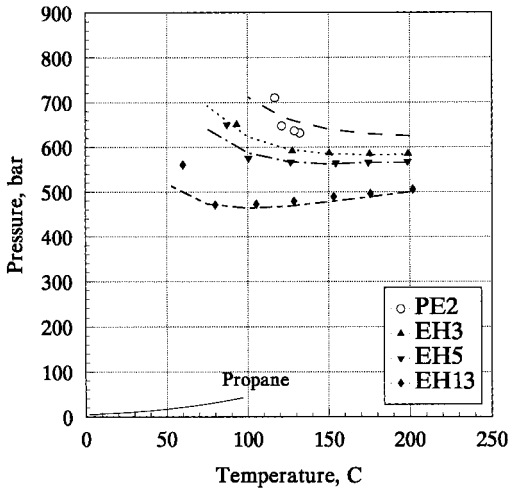

Figure 8. Cloud-point pressures of EH copolymers in propane (5 wt %). The curves are calculated from the copolymer SAFT equation of state. The solid line is the vapor pressure of propane.

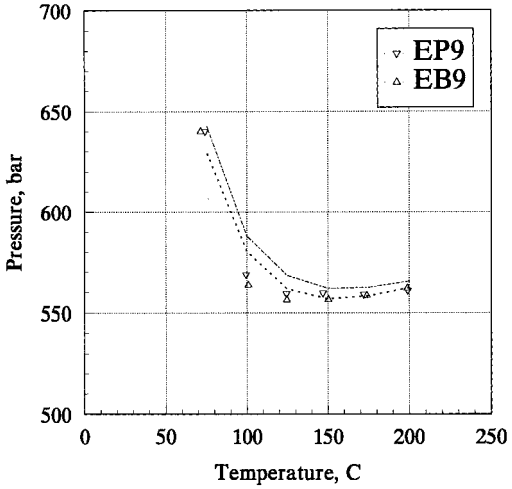

Figure 9. Cloud-point pressures of EP9 and EB9 in propane (5 wt %). The curves are calculated from the copolymer SAFT equation of state.

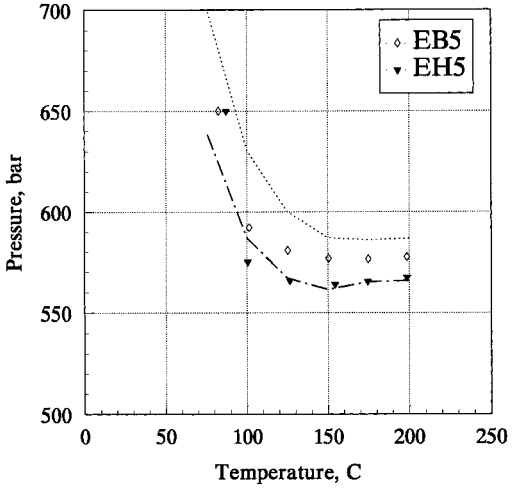

Figure 10. Cloud-point pressures of EH5 and EB5 in propane (5 wt %). The curves are calculated from the copolymer SAFT equation of state.

solid−liquid transition is reversible upon heating the solution while the cloud-point (liquid−liquid transition) is reversible on heating or pressurizing the solution.

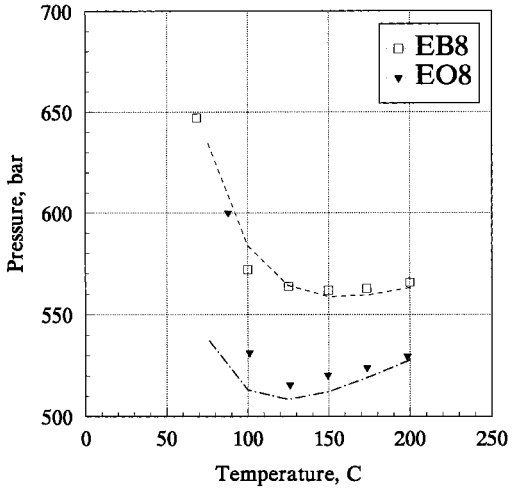

Figure 11. Cloud-point pressure of EO8 and EB8 copolymers in propane (5 wt %). The curves are calculated from the copolymer SAFT equation of state.

Table 4. Solid-Liquid Transitions of Ethylene Copolymers in Propane

polymer (concn, wt %)	temp, °C	pressure, bar	polymer (concn, wt %)	temp, °C	pressure, bar
PE1 (1)	106.0	642.5	EB9 (5)	71.6	640.4
EP9 (5)	74.3	640.0	EB16 (5)	44.8	625.0
EP10 (5)	62.3	613.1	EB18 (5)	57.3	630.0
EP28 (5)	38.0	550.0	EH3 (5)	93.2	650.0
EP100 (5)	65.8	540.0	EH5 (5)	87.2	650.0
EB5 (5)	82.5	650.0	EH13 (5)	60.0	560.0
EB8 (5)	68.5	647.0	EO8 (5)	88.0	600.0

Figure 6 shows a similar effect of the ethyl branches on the cloud-point pressures of the EB copolymers in 1 wt % solutions in propane. The cloud-point pressures decrease as the ethyl branch content increases, which is captured by copolymer SAFT. Furthermore, the UCST type phase behavior changes to LCST type phase behavior as the number of ethyl branches in the EB copolymer increases. A few measured solid−liquid transitions are indicated in Table 4. Similar patterns are observed for 5 wt % EB solutions in propane, as shown in Figure 7. EH solutions in propane also resulted in similar patterns such as EB solutions, as shown in Figure 8. As the butyl branch fraction increases, the cloud-point pressures decrease.

This general pattern of how the increasing branch content decreases the cloud-point pressure can be explained on the basis of a "like-dissolve-like" principle: Increasing branch content decreases the copolymer density, intermolecular energy, and cohesive energy density; it makes them more similar to those of propane.

Figures 9−11 illustrate a weak effect of the branch length on the cloud-point pressure. For example, the cloud-point pressures between 100 and 200 °C and the solid−liquid transition temperatures for EP9 and EB9 nearly coincide. As we increase the difference in the branch length, by comparing EB5 and EH5 (ethyl to butyl) and EB8 and EO8 (ethyl to hexyl), we find that increasing branch length tends to decrease the cloud-point pressure. This pattern is consistent with the difference in the solubility parameter values. The solubility parameter values of EP9 and EB9 are very close to each other so that the solubility in propane is substantially identical. However, the solubility parameter of EO8 is lower than EB8 so that EO8 is more soluble than EB8 in propane.

Copolymer SAFT correlation indicates that the estimated branch segment energies of EP, EB, and EH copolymers are constant except for EP100 and EB23. It also shows the segment energies increase as the branch lengths increase. The branch segment energies are lower than the backbone segment energy in all cases. These suggest that the branch segment energy can be used as a fitting parameter of copolymer SAFT to the experimental data.

Conclusions

The cloud-point pressures of ethylene−propylene, ethylene−butene, ethylene−hexene, and ethylene−octene copolymer solutions in subcritical and supercritical propane, are found to decrease with increasing branch content. At the same branch content, the cloud-point pressures of EP and EB copolymers in propane are found to coincide. As the branch length increases, however, the cloud-point pressures tend to decrease slightly. The copolymer SAFT equation of state is found to account well for these short chain branching effects by adjusting the branch segment energy.

Supporting Information Available: Tabulated experimental data taken in this work for EP's, EB's, EH's, and EO, in a high-pressure batch cell (4 pages). Ordering information is given on any current masthead page.

Acknowledgment. M. Radosz acknowledges the U.S. Department of Energy Grant No. DE-FG 02-96ER12201.

References and Notes

(1) Spahl, R.; Luft, G. *Ber. Bunsen-Ges. Phys. Chem*. **1982**, *86*, 621.
(2) Chen, S. J.; Banaszak, M.; Radosz, M. *Macromolecules* **1995**, *28*, 1812.
(3) De Loos, T. W.; Poot, W.; Lichtenthaler, R. N. *J. Supercrit. Fluids* **1995**, *8*, 282.
(4) Charlet, G.; Delmas, G. *Polymer* **1981**, *22*, 1181.
(5) Whaley, P. D.; Winter, H. H.; Ehrlich, P. *Macromolecules* **1997**, *30*, 4887.
(6) Hamielec, A. E.; Soares, J. B. P. *Prog. Polym. Sci*. **1996**, *21*, 651.
(7) Welborn, H. C.; Speed, C. S. U.S. Patent 5, 084, 534, Jan. 28, 1992.
(8) Wertheim, M. S. *J. Chem. Phys*. **1986**, *87*, 7323.
(9) Condo, P. D.; Raodsz, M. *Fluid Phase Equilib*. **1996**, *117*, 1.
(10) Banaszak, M.; Chen, C. K.; Radosz, M. *Macromolecules* **1996**, *29*, 6481.
(11) Huang, S. H.; Radosz, M. *Ind. Eng. Chem. Res*. **1990**, *29*, 2284.
(12) Chen, S.-j.; Chiew, Y. W.; Gardecki, J. A.; Nilsen, S.; Radosz, M. *J. Polym. Sci., Polym. Phys.* **1994**, *32*, 1791.
(13) Chen, C. K.; Duran, M. A.; Radosz, M. *Ind. Eng. Chem. Res.* **1993**, *32*, 3123.
(14) Balsara, N. P.; Fetters, L. J., Hadjichristidis, N.; Lohse, D. J.; Han, C. C.; Graessley, W. W.; Krishnamoorti, R. *Macromolecules* **1992**, *25*, 6137.
(15) Graessley, W. W.; Krishnamoorti, R.; Balsara, N. P.; Butera, R. J.; Fetters, L. J.; Lohse, D. J.; Schulz, D. N.; Sissano, J. A. *Macromolecules* **1994**, *27*, 3896.
(16) Chen, S. J.; Randelman, R. E.; Seldomridge, R. L.; Radosz, M. *J. Chem. Eng. Data* **1993**, *38*, 2121.
(17) Condo, P. D.; Colman, E. J.; Ehrlich, P. *Macromolecules* **1992**, *25*, 750.

MA971579X